

MeV N⁺-ion irradiation effects on α -MoO₃ thin films

R. Sivakumar

Institute of Physics, Sachivalaya Marg, Bhubaneswar 751 005, India

C. Sanjeeviraja

Department of Physics, Alagappa University, Karaikudi 630 003, India

M. Jayachandran

ECMS Division, Central Electrochemical Research Institute, Karaikudi 630 006, India

R. Gopalakrishnan

Department of Physics, Anna University, Chennai 600 025, India

S. N. Sarangi, D. Paramanik, and T. Som^{a)}

Institute of Physics, Sachivalaya Marg, Bhubaneswar 751 005, India

(Received 6 October 2006; accepted 19 December 2006; published online 14 February 2007)

In this work, modifications in the structural, vibrational, optical, and surface morphological properties of 2 MeV N⁺-ion irradiated α -MoO₃ thin films are studied. Nitrogen irradiation up to the fluence of 1×10^{15} ions cm⁻² does not lead to any structural phase change. The irradiation induced formation of nanoscale defect structures at the film surface becomes more prominent at higher irradiation fluences, leading to the enhancement in the optical absorption behavior of the irradiated films. The possible role of energy loss process in the mechanism of modifying the surface morphology has been discussed. © 2007 American Institute of Physics. [DOI: [10.1063/1.2437656](https://doi.org/10.1063/1.2437656)]

I. INTRODUCTION

The transition metal oxides have attracted the attention of many researchers during the last few years because of their technological applications in the fields of microelectronics, solid-state microbatteries, and optoelectronics.¹⁻³ Molybdenum trioxide (MoO₃) is one among these with a vast potential in developing positive alpha-numeric display devices, high density memory devices, optical smart windows, and solid-state microbatteries.⁴⁻⁶ This is possible because MoO₃ in the orthorhombic phase has a unique layered structure, high chemical stability, and interesting electrochemical properties.⁷ In addition, this material also exhibits photochromic and thermochromic properties.^{8,9} Several growth techniques such as thermal evaporation,¹⁰ electron-beam evaporation,¹¹ and sputtering^{7,12} are typically employed for deposition of MoO₃ films. The optical properties of MoO₃ films can be varied by dc injection, ultraviolet irradiation, and exposure to atomic hydrogen or molecular hydrogen gas in contact with a catalyst, irradiation by a beam of ions or electrons, or heating.³

Ion irradiation is a useful tool for impurity doping and defect production in materials, which helps to alter their structural, electrical, optical, and magnetic properties with a high spatial selectivity.^{13,14} Irradiation induced changes brought about on the surface morphology of materials also play a significant role in the case of device fabrication. Hirata *et al.* studied the hydrogen related changes in the structural property of proton implanted MoO₃ films by Raman scattering.¹⁵ However, no attempt has been made to understand the effects of ion irradiation on the structural, opti-

cal, and surface morphological properties of MoO₃ thin films grown by electron-beam evaporation technique. These studies can be useful in assessing the viability of using MoO₃ thin film based devices in radiation harsh environments.

In this paper, we investigate the effects of MeV N⁺-ion irradiation on electron-beam evaporated thin MoO₃ films grown at room temperature (RT). The results are attributed to the fact that high-energy N⁺-ion irradiation enhances the optical absorption behavior of MoO₃ films and modifies the energy band gap. This supports our results on vibrational and surface morphological properties of irradiated thin MoO₃ films.

II. EXPERIMENT

The MoO₃ films were deposited on clean Corning 7059 microscopic glass substrates under a chamber pressure of 1×10^{-5} mbar at RT. The thickness of the deposited film was about 1.32 μ m. Later on, these films were irradiated at RT by using 2 MeV N⁺ ions to the fluences of 1×10^{12} , 1×10^{13} , 1×10^{14} , and 1×10^{15} ions cm⁻². Monte Carlo SRIM-2003 simulation predicts the projected range of the N ions in the MoO₃ films to be 1400 nm, and hence the ions are expected to penetrate into the substrate.¹⁶ The nuclear energy loss (S_n) and the electronic energy loss (S_e) values in the MoO₃ films corresponding to the 2 MeV nitrogen ions are 1.2×10^{-4} and 1.9×10^{-2} keV nm⁻¹, respectively, as obtained from SRIM-2003 calculations.¹⁶ Since the S_e value is two orders of magnitude larger than the S_n value, the incident N⁺ ions lose energy predominantly via inelastic collisions with the target electrons.

Phase analysis of the pristine and the N⁺ irradiated MoO₃ films was performed by x-ray diffraction (XRD) studies using the Cu $K\alpha$ radiation ($\lambda=0.154$ nm) over a 2θ scan

^{a)}Author to whom correspondence should be addressed; FAX: +91-674-2300142; electronic mail: tsom@iopb.res.in

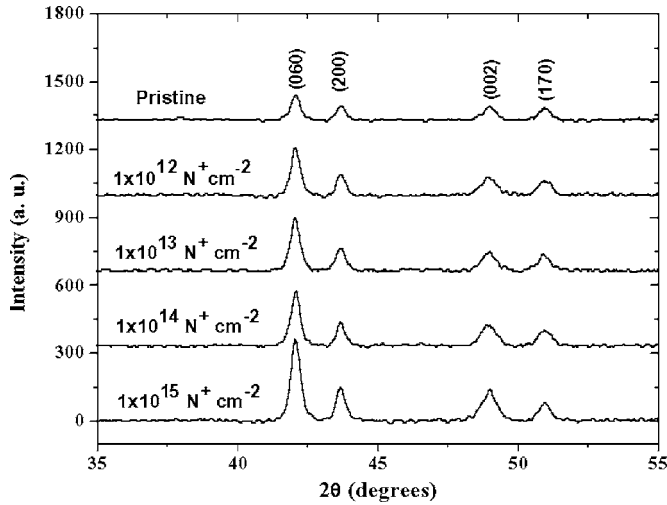


FIG. 1. X-ray diffraction patterns of MoO₃ films before and after 2 MeV nitrogen-ion irradiation to various fluences.

range of 35°–55°. The optical absorption spectra were recorded using an UV-Vis-NIR (Vis and NIR denotes visible and near infrared, respectively) spectrophotometer in the range of 300–1100 nm. Micro-Raman measurements were performed at RT using a backscattering geometry. The spectra were recorded using the 514.5 nm line of Ar⁺-ion laser with a 200 mW power and over a 10 μm spot size. Irradiation induced changes in the surface morphology of the films were studied by atomic force microscopy (AFM).

III. RESULTS AND DISCUSSION

Figure 1 shows the XRD patterns of the pristine MoO₃ films irradiated with nitrogen ions at RT. It shows that the MoO₃ films before and after the irradiation are polycrystalline in nature and the observed *d* spacings match closely with the orthorhombic structure (α phase).¹⁷ This indicates that no major structural phase change occurs in the MoO₃ films due to irradiation even up to the maximum fluence of 1×10^{15} ions cm⁻², which is similar to the results observed for H⁺ implanted MoO₃ films.¹⁵ Further, no substantial change in the lattice parameters ($a=0.396$ nm, $b=1.385$ nm, and $c=0.369$ nm) takes place for the films irradiated up to the highest fluence.¹⁷ This negligible change in lattice parameters implies only the slight distortion of the Mo–O framework upon nitrogen-ion irradiation. However, the increasing peak intensity and narrowing of the peaks could be indicative of irradiation induced grain growth. It is observed from Fig. 2 that an increase in crystallite size (*D*) and the decreasing dislocation density (δ) of the predominant peak [(060)] are evident with increasing ion fluence. It may be mentioned here that *D* is defined as $0.94\lambda/\beta \cos \theta$, where β is the full width at half maximum (in radians) of the XRD peak and δ is defined as $1/D^2$.^{18,19} Normally, during ion irradiation, two competing processes occur simultaneously, one is the generation of vacancies, agglomeration of vacancies and then collapsing into dislocation loops, and the other is their annihilation at the possible sinks. With increasing ion fluence, though more vacancies are created, annihilation rate of va-

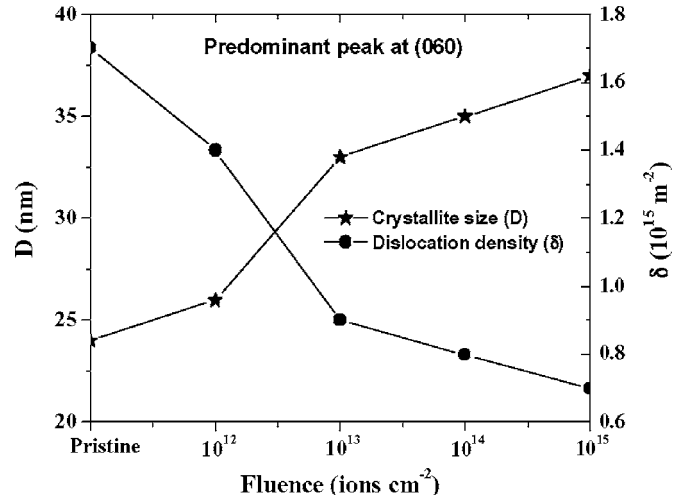


FIG. 2. Variation in the crystallite size (*D*) and the dislocation density (δ) vs N⁺-ion fluence for MoO₃ films.

cancies also increases as the sink density increases with irradiation. Hence, a decrease in the dislocation density is observed with increasing ion fluence.

The optical absorption spectra of the pristine and the irradiated films are shown in Fig. 3. It is seen that there is an increase in the optical absorption with increasing N-ion fluence, which is caused by the free-carrier absorption corresponding to the increase in the conductivity.^{20,21} It is also clear from the spectra that the absorption edges shift towards the higher wavelengths, indicating a systematic reduction in the optical band gap with increasing ion fluence. It may be mentioned that MoO₃ is a direct band gap system and hence the plot of $(ah\nu)^2$ vs $E(=h\nu)$ (known as the “Tauc plot”) is expected to show a linear behavior in the higher energy region which corresponds to a strong absorption near the absorption edge. Extrapolating the linear portion to zero absorption edge results to the optical energy band gap of the films. From Fig. 3 we observe the absorption edge at nearly 400 nm. Thus, we get the linear portion in the Tauc plot corresponding to the data in the range of 400–500 nm. This

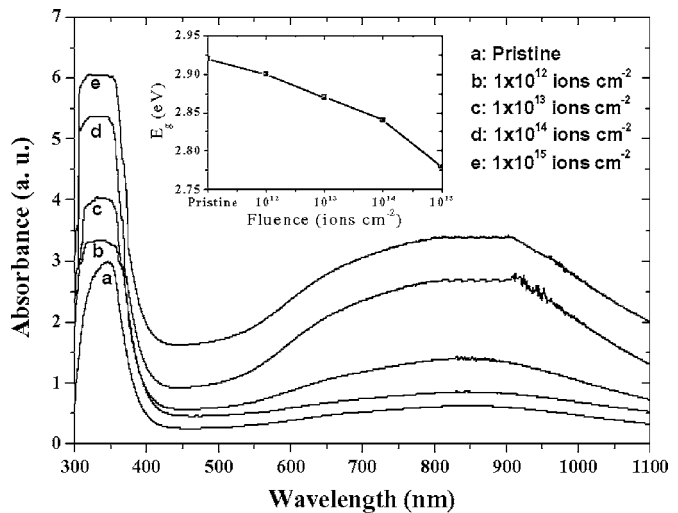


FIG. 3. Optical absorption spectra of the MoO₃ films before and after nitrogen irradiation at different fluences.

gives rise to the band gap value of the pristine film to be 2.92 eV (425 nm). Likewise, the band gaps at different N-ion fluences are calculated. The observed values are 2.90, 2.87, 2.84, and 2.78 eV, respectively, for the films irradiated with fluences of 1×10^{12} , 1×10^{13} , 1×10^{14} , and 1×10^{15} ions cm^{-2} , respectively. The reduction in the optical band gap with increasing ion fluence is shown as the inset of Fig. 3. This trend indicates that the top of the valence band and the bottom of the conduction band are modified to various extents with increasing ion fluence.

It is known that ion irradiation produces point defects such as vacancies, antisite defects, and interstitials causing lattice damage. Hence, the reduction in the band gap with increasing ion fluence may arise due to the effect of band tailing, owing to the defects produced during irradiation. In fact, the high-energy ions excite the electrons from both the lone pair and bonding states to the higher energy states. Vacancies created in these states are immediately filled by the outer electrons with Auger processes that in turn induce more holes in the lone pair and bonding orbital, leading to a vacancy cascade process. In this process, MeV N-ion induced defects produce localized states near the band edges which in turn modify the MoO_3 band structure.

The observed redshift in the absorption edges of irradiated MoO_3 films may also be correlated with the coalescence of small crystallites into effectively larger crystallites but at the same time retaining the nanostructure morphology of the film surfaces. The reduction in the optical band gap with ion fluence is also in conformity with the report of Julien *et al.*²² where they observe a decrease in the band gap of MoO_3 films with increasing substrate temperature (during film growth). It has also been reported that the increasing substrate temperature leads to the enhancement in crystallite size and the intensities of XRD peaks of MoO_3 .²² This is consistent with our XRD analysis where an increased grain growth of irradiated films with increasing N^+ -ion fluence can be observed, as explicitly seen from the decrease in full width at half maximum of (060), (200), (002), and (170) peaks (Fig. 1).

The Raman spectra of the MoO_3 films before and after nitrogen-ion irradiation are shown in Fig. 4. The crystalline nature of the pristine film is clearly visible from the well defined Raman peaks, which are in good agreement with the previous reports.^{15,23,24} As the molybdenum atom is about six times heavier than the oxygen atom, the vibrations of the system are supposed to involve mainly the lighter oxygen atoms in the present crystal lattice system. In addition, $\alpha\text{-MoO}_3$ is made up of distorted MoO_6 octahedra with Mo–O bond lengths ranging from 0.17 to 0.23 nm. This leads to a marked differentiation in the positioning of individual oxygen atom in terms of their site symmetry. As a result, in each octahedron, one oxygen atom remains unshared (Mo=O), while the two axial oxygen atoms are common to two octahedra (Mo–O–Mo) and the three other equatorial ones are common to three octahedra (OMo_3).²⁵ The observed broad peak at 666 cm^{-1} corresponds to the stretching of the bridging oxygen of OMo_3 units and is a characteristic one for the orthorhombic molybdenum oxide ($\alpha\text{-MoO}_3$) structure.²⁴ These (O– Mo_3) groups are planar

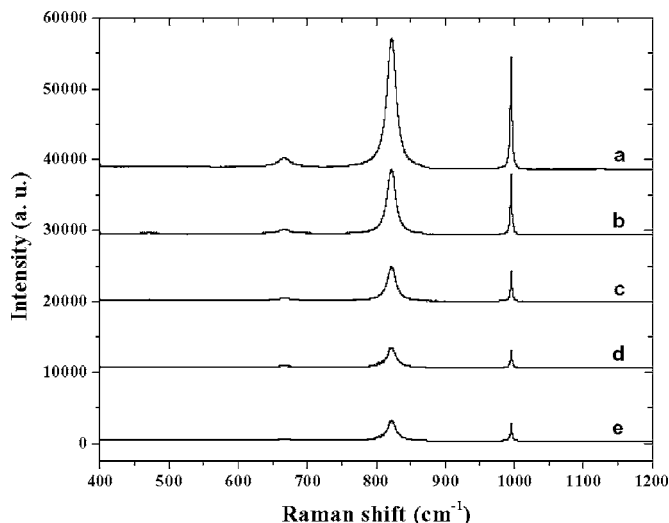


FIG. 4. Micro-Raman spectra of the MoO_3 films: (a) Before and after nitrogen irradiation to various fluences: (b) 1×10^{12} ions cm^{-2} , (c) 1×10^{13} ions cm^{-2} , (d) 1×10^{14} ions cm^{-2} , and (e) 1×10^{15} ions cm^{-2} .

type in MoO_3 which reduces the symmetry of the basic octahedron. The strong line at 822 cm^{-1} corresponds to the stretching vibrations of Mo–O–Mo bonding in $\alpha\text{-MoO}_3$. The Raman-active band at 995 cm^{-1} is attributed to the stretching mode of the Mo–O and this peak is associated with the unique molybdenyl bond, which is responsible for the layered structure of $\alpha\text{-MoO}_3$.

Comparing the Raman spectra of the pristine sample and those of the irradiated ones, it is clear that the shift in the peak positions is rather insignificant. However, the relative intensity (peak height) of the Raman lines decreases with increasing ion fluence. This can be interpreted based on the electronic screening of phonons in conjunction with intra-band activity within the framework of the proposed band structure in the metallic state.¹⁵ In addition, the Raman peak widths also increase (as shown in Fig. 4), since the phonon lifetime is found to reduce whenever an increase in defect density is effected in the crystal lattice.

Figure 5 shows the variation in the area under the different Raman peaks of the MoO_3 films. The area under all the

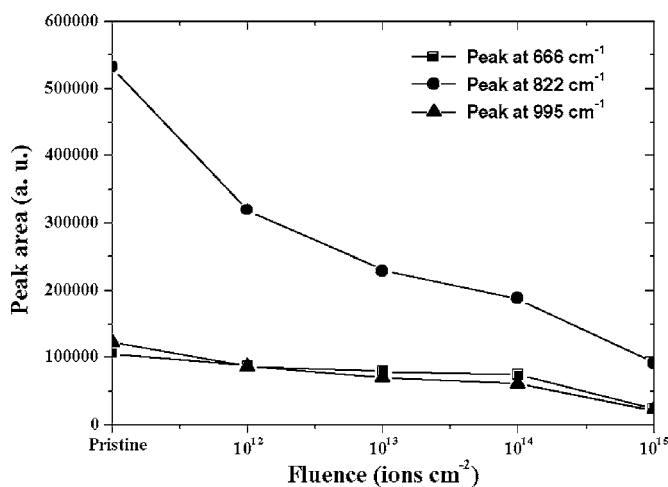


FIG. 5. Variation in the Raman peak area vs nitrogen-ion fluence for the MoO_3 films.

Raman peaks decreases with increasing ion fluence. The area under a Raman line may reduce due to irradiation induced lattice disorder²⁶ which is consistent with our optical studies where the band gap reduces with increasing fluence. This is attributed to deterioration in the translational symmetry of the MoO₃ crystal due to ion induced defects, which relaxes the k -conservation rule for the Raman transition corresponding to the MoO₃ peak.

Figure 6 shows the three-dimensional AFM images (500 × 500 nm²) of the pristine and the N⁺-ion irradiated MoO₃ films. The AFM image of the pristine sample [Fig. 6(a)] indicates the growth of a uniform granular film at RT. Irradiation of the films causes the following notable changes in the surface morphology: (i) the boundary between the grains tends to smear out and (ii) large mounds and pits appear on the surface [Figs. 6(b) and 6(c)]. In fact, the AFM images (not shown) for the other two fluences also show similar morphological changes. This is followed by an increase in the rms surface roughness of the films with fluence. For example, the average rms surface roughness of the pristine sample is 0.8 nm and it increases up to 4.7 nm for the irradiated films at the fluence of 1×10^{15} ions cm⁻².

As mentioned earlier, the effects of 2 MeV nitrogen ions would be governed by the electronic excitation. Normally, it is expected that the electronic excitation will not cause much movement of atoms because it either results in the excitation or ionization. However, MoO₃ films being insulating in nature, according to the Coulomb explosion model, the positive charges generated by the incident ion along its path may cause atomic motion due to the Coulomb force.²⁷ In fact, using the SRIM-2003 code, it is found that the sputtering yields for Mo and O atoms are extremely small (Mo: 0.007 at. ion⁻¹ and O: 0.05 at. ion⁻¹) at these energies. In addition, the surface features do not resemble the ion induced surface rippling since it is unexpected to see ripples with the present ion energy, fluence, and the geometry.²⁸ Therefore, the increasing surface roughness of the films can be attributed to atomic movements caused due to N-ion irradiation.

IV. CONCLUSIONS

In summary, nitrogen-ion irradiation induced changes in the structural, optical, vibrational, and surface morphological properties of molybdenum oxide (MoO₃) thin films were examined. XRD measurements of the irradiated films reveal irradiation induced grain growth and reduction in the dislocation density. A systematic reduction in the optical band gap is observed with increasing ion fluence, which is associated with N-ion induced defects leading to the production of localized states near the band edges and in the energy gap of MoO₃. The reduction in the Raman-active band at 995 cm⁻¹ is attributed to the destruction of the layered structure in α -MoO₃. Further, the area under the Raman peaks decreases with increasing ion fluence, which is attributed to deterioration of the translation symmetry in MoO₃ lattice due to ion induced defects. AFM studies show increasing surface roughness of the films at higher fluences due to irradiation induced atomic motion.

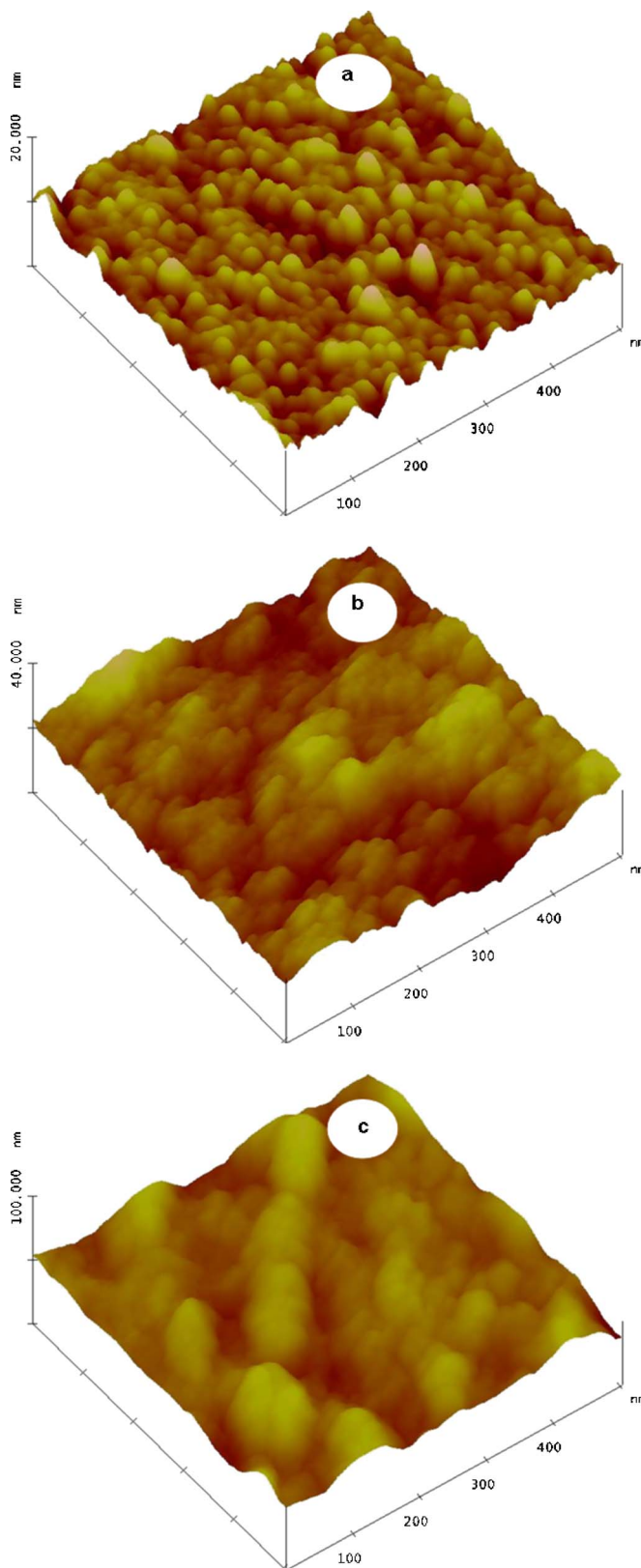


FIG. 6. (Color online) AFM images of the MoO₃ films: (a) Before and after nitrogen irradiation to various fluences: (b) 1×10^{13} N⁺/cm² and (c) 1×10^{15} N⁺/cm².

ACKNOWLEDGMENTS

Thanks are due to Dr. S. N. Sahu for extending the Raman scattering and optical absorption facilities. Dr. S. Varma is acknowledged for extending the AFM facility.

- ¹A. K. Arof, E. B. Sariman, and M. Z. Mastor, *J. Phys. III* **4**, 849 (1994).
- ²C. Julien, B. Yebka, and J. P. Guesdon, *Ionics* **1**, 316 (1995).
- ³C. G. Granqvist, *Handbook of Inorganic Electrochromic Materials* (Elsevier, Amsterdam, 1995).
- ⁴A. Donnadieu, *Mater. Sci. Eng., B* **3**, 185 (1989).
- ⁵C. Julien, L. El-Farh, M. Balkanski, O. M. Hussain, and G. A. Nazri, *Appl. Surf. Sci.* **65–66**, 325 (1993).
- ⁶D. W. Murphy, P. A. Christian, F. J. Disalvo, and J. N. Canides, *J. Electrochem. Soc.* **126**, 497 (1979).
- ⁷O. M. Hussain, K. Srinivasa Rao, K. V. Madhuri, C. V. Ramana, B. S. Naidu, S. Pai, J. John, and R. Pinto, *Appl. Phys. A: Mater. Sci. Process.* **75**, 417 (2002).
- ⁸J. Scarminio, A. Lourenco, and A. Gorenstein, *Thin Solid Films* **302**, 66 (1997).
- ⁹M. A. Quevedo Lopez, R. Ramirez-Bon, R. A. Orozco-Teran, O. Mendoza-Gonzalez, and O. Zeleya-Angel, *Thin Solid Films* **343**, 202 (1999).
- ¹⁰C. Julien, O. M. Hussain, L. El-Farh, and M. Balkanski, *Solid State Ionics* **53–56**, 400 (1992).
- ¹¹R. Sivakumar, V. Vijayan, V. Ganesan, M. Jayachandran, and C. Sanjeeviraja, *Smart Mater. Struct.* **14**, 1204 (2005); R. Sivakumar, P. Manisankar, M. Jayachandran, and C. Sanjeeviraja, *Sol. Energy Mater. Sol. Cells* **90**, 2438 (2006).
- ¹²W. Gulbinski, D. Pailhavey, T. Suszko, and Y. Mathey, *Appl. Surf. Sci.* **475**, 149 (2001).
- ¹³J. S. Williams and J. M. Poate, *Ion Implantation and Beam Process* (Academic, New York, 1984); P. D. Townsend, P. J. Chandler, and L. Zhang, *Optical Effects of Ion Implantation* (Cambridge University Press, Cambridge, 1994).
- ¹⁴S. Ghosh, M. Mäder, R. Grötzschel, A. Gupta, and T. Som, *Appl. Phys. Lett.* **89**, 104104 (2006).
- ¹⁵T. Hirata, K. Ishioka, and M. Kitajima, *Appl. Phys. Lett.* **68**, 458 (1996).
- ¹⁶<http://www.srim.org/>.
- ¹⁷JCPDS-International Center for Diffraction Data, Powder Diffraction File No. 05-0508 (ICDD, Newton Square, PA, 2000).
- ¹⁸G. B. Williamson and R. C. Smallman, *Philos. Mag.* **1**, 34 (1956).
- ¹⁹S. Gopal, C. Viswanathan, B. Karunakaran, Sa. K. Narayandass, D. Mangalaraj, and J. Yi, *Cryst. Res. Technol.* **40**, 557 (2005).
- ²⁰J. S. E. M. Svensson and C. G. Granqvist, *Appl. Phys. Lett.* **45**, 828 (1984).
- ²¹T. J. Tate, M. Garcia-Parajo, and M. Green, *J. Appl. Phys.* **70**, 3509 (1991).
- ²²C. Julien, A. Khelifa, O. M. Hussain, and G. A. Nazri, *J. Cryst. Growth* **156**, 235 (1995).
- ²³L. Seguin, M. Figlarz, R. Cavagnat, and J. C. Lassegues, *Spectrochim. Acta, Part A* **51**, 1323 (1995).
- ²⁴K. A. Gesheva, T. Ivanova, and F. Hamelmann, *Sol. Energy Mater. Sol. Cells* **90**, 2532 (2006).
- ²⁵I. R. Beattie and T. R. Gilson, *J. Chem. Soc. A* **1969**, 2322.
- ²⁶T. Motooka and O. W. Holland, *Appl. Phys. Lett.* **61**, 3005 (1992).
- ²⁷R. L. Fleischer, P. B. Price, and R. M. Walker, *J. Appl. Phys.* **36**, 3645 (1965).
- ²⁸D. P. Dutta and T. K. Chini, *Phys. Rev. B* **71**, 235308 (2005); L. Ling, W. Li, L. Qi, M. Lu, X. Yang, and C. Gu, *ibid.* **71**, 155329 (2005).